TABLE 2 Hotspot and coldspot overlap data

		Hotspots				
(*a*) Hotspot overlap and coldspot overlap						
	—	Butterflies	Dragonflies	Liverworts	Aquatic plants	Breeding Birds
	Butterflies	—	0.34 ($n=99$)	0.0 ($n=101$)	0.6 ($n=118$)	0.26 ($n=112$)
	Dragonflies	0.24 ($n=89$)	—	0.0 ($n=94$)	0.25 ($n=111$)	0.12 ($n=116$)
Coldspots	Liverworts	0.13 ($n=29$)	0.09 ($n=145$)	—	0.03 ($n=98$)	0.23 ($n=116$)
	Aquatic plants	0.13 ($n=111$)	0.16 ($n=170$)	0.11 ($n=142$)	—	0.21 ($n=112$)
	Breeding birds	0.15 ($n=115$)	0.22 ($n=88$)	0.14 ($n=94$)	0.21 ($n=58$)	—
(*b*) Hotspot overlap with coldspots						
	Butterflies	—	0.00 ($n=99$)	0.28 ($n=29$)	0.01 ($n=111$)	0.01 ($n=116$)
	Dragonflies	0.02 ($n=108$)	—	0.01 ($n=94$)	0.02 ($n=111$)	0.02 ($n=114$)
Coldspots	Liverworts	0.04 ($n=115$)	0.07 ($n=107$)	—	0.09 ($n=109$)	0.01 ($n=104$)
	Aquatic plants	0.08 ($n=118$)	0.02 ($n=111$)	0.11 ($n=98$)	—	0.03 ($n=112$)
	Breeding birds	0.0 ($n=115$)	0.03 ($n=88$)	0.07 ($n=94$)	0.0 ($n=58$)	—
(c) Taxon representation in hotspots						
	X↓ Y→	Butterflies	Dragonflies	Liverworts	Aquatic plants	Breeding birds
	Butterflies	0.91	0.91	0.64	0.82	1
	Dragonflies	0.82	0.92	0.72	1	0.92
	Liverworts	0.48	0.57	0.95	0.69	0.92
	Aquatic plants	0.86	0.88	0.91	0.96	0.94
	Breeding birds	0.7	0.73	0.75	0.88	0.87

a, Proportional overlap of hotspots with hotspots (top right) and hotspots with coldspots (bottom left) for each group, n = maximum possible number of overlaps, calculated as the smaller of the pair of hotspot groups adjusted for squares lacking records for either group. For example there are 123 butterfly hotspots and 107 liverwort hotspots; therefore the maximum possible overlap between these two groups is 107 squares. Of these, six liverwort hotspots lie in squares unrecorded for butterflies and are therefore excluded. Thus the actual maximum possible overlap for these groups is 101 squares. *b*, Proportional overlap of hotspots with coldspots for each group, n = maximum possible number of overlaps, calculated as above. Note that two values are shown for each pair of taxa. Thus, overlap between coldspots of butterflies with hotspots of liverworts is 0.28 but that of hotspots of butterflies with coldspots of liverworts is 0.04. *c*, Proportion of the species in the taxa listed in column X occurring in the full set of hotspots identified for the taxa in row Y (for example, 91% of the British butterfly species occur in the 123 squares identified as butterfly hotspots; the same 123 butterfly hotspots contain 82% of all the British dragonfly species, 48% of liverworts and so on).

criteria, diversity (species richness) and rarity, and on only one or a limited number of taxa, may fail to provide adequate protection for many other organisms. □

Received 30 April; accepted 12 July 1993.

1. Soulé, M. (ed.) *Conservation Biology* (Sinauer, Sunderland, Mass., 1986).
2. Groombridge, B. (ed.) *Global Diversity: Status of the Earth's Living Resources* (Chapman & Hall, London, 1992).
3. Pressey, R. L., Humphries, C. J., Margules, C. R., Vane-Wright, R. I. & Williams, P. H. *Trends Ecol. Evol.* **8,** 124–128 (1993).
4. Raven, P. H. & Wilson, E. O. *Science*, **258,** 1099–1100 (1992).
5. Pearson, D. L. & Cassola, F. *Cons. Biol.* **6,** 376–391 (1992).
6. Margules, C. & Usher, M. B. *Biol. Conserv.* **21,** 79–109 (1981).
7. Usher, M. B. (ed.) *Wildlife Conservation Evaluation* (Chapman & Hall, London, 1986).
8. Scott, M. J. *et al. Wildl. Monogr.* **123,** 1–41 (1993).
9. Harding, P. T. & Sheail, J. *Biological Recording of Changes in British Wildlife* (ed. Harding, P. T.) 5–19 (HMSO, London, 1992).
10. Myers, N. *The Environmentalist* **8,** 187–208 (1988).
11. Kremen, C. *Ecol. Appl.* **2,** 203–217 (1992).
12. Rorslett, B. *Aquat. Bot.* **39,** 173–179 (1991).
13. Williams, P. H. & Gaston, K. J. *Biol. Conserv.* (in the press).
14. Dury, W. H. *Biol. Conserv.* **6,** 162–169 (1974).
15. Rabinowitz, D. *Biological Aspects of Rare Plant Conservation* (ed. Synge, H.) 205–217 (Wiley, New York, 1981).
16. Thomas, C. D. & Mallorie, H. C. *Biol. Conserv.* **33,** 95–117 (1985).
17. Perring, F. H. & Farrell, L. *British Red Data Books: 1, Vascular Plants* 2nd edn (RSNC, Nettleham, 1983).
18. Stewart, A. & Pearman, D. *BSBI (Botanical Society of the British Isles) News* **57,** 17–21 (1991).
19. International Council for Bird Preservation *Putting Biodiversity on the Map: Priority Areas for Global Conservation* (International Council for Bird Preservation, Cambridge, 1992).
20. Vane-Wright, R. I., Humphries, C. J. & Williams, P. H. *Biol. Conserv.* **55,** 235–254 (1991).
21. Crozier, R. H. *Biol. Conserv.* **61,** 11–15 (1992).
22. Gibbons, D. W., Reid, J. B. & Chapman, R. A. *The New Atlas of Breeding Birds in Britain and Ireland: 1988–91* (in the press).
23. Prendergast, J. R., Wood, S. N., Lawton, J. H. & Eversham, B. C. *Biodiversity Lett.* (in the press).

ACKNOWLEDGEMENTS. We thank the volunteer recorders who provided all the distribution data and S. Naeem and R. I. Vane-Wright for helpful comments on the manuscript. Maps were produced by the DMAP program, written by Alan Morton, Imperial College. The Centre for Population Biology and the BRC are funded by the Natural Environment Research Council (NERC). The New Atlas of Breeding Birds in Britain and Ireland: 1988–91 (BTO) was funded initially by the Central Electricity Generating Board and subsequently by its four successors: National Grid Company, National Power, PowerGen and Nuclear Electric, additional funding was provided by the Nature Conservancy Council and subsequently by the Joint Nature Conservation Committee. J.R.P. is supported by a NERC studentship; R.M.Q. is supported by a NERC Special Topics Studentship from the Esmée Fairbairn Trust, both CASE awards with the Institute of Terrestrial Ecology.

Noise enhancement of information transfer in crayfish mechanoreceptors by stochastic resonance

John K. Douglass*‡, Lon Wilkens*, Eleni Pantazelou† & Frank Moss*†§

Departments of * Biology and † Physics, University of Missouri at St Louis, St Louis, Missouri 63121, USA

In linear information theory, electrical engineering and neurobiology, random noise has traditionally been viewed as a detriment to information transmission. Stochastic resonance (SR) is a nonlinear, statistical dynamics whereby information flow in a multistate system is enhanced by the presence of optimized, random noise[1–4]. A major consequence of SR for signal reception is that it makes possible substantial improvements in the detection of weak periodic signals. Although SR has recently been demonstrated in several artificial physical systems[5,6], it may also occur naturally, and an intriguing possibility is that biological systems have evolved the capability to exploit SR by optimizing endogenous sources of noise. Sensory systems are an obvious place to look for SR, as they excel at detecting weak signals in a noisy environment. Here we demonstrate SR using external noise applied to crayfish mechanoreceptor cells. Our results show that individual neurons can provide a physiological substrate for SR in sensory systems.

The concept of SR originated in efforts to explain the suggested periodicities in recurrences of the Earth's ice ages as the

§ To whom correspondence should be addressed.
‡ Present address: ARL Division of Neurobiology, University of Arizona, Tucson, Arizona 85721, USA.

result of stochastic and weak periodic forces acting in concert on a bistable, global climate model[7–10]. Subsequent experimental[1] and theoretical[2,3] work demonstrated that the information content of a weak signal can be maximized by noise in certain nonlinear systems. An operational definition of SR is that some measure of the output coherence relative to the output noise passes through a maximum at an optimal value of the input noise.

As a preliminary search for SR in living systems, we have studied the timing of spiking events (action potentials) in single mechanoreceptor cells of the crayfish, *Procambarus clarkii*[11–13]. As spiking can be induced by both noise and a coherent signal, we hypothesized that transmission of a weak mechanical stimulus could be enhanced by an optimal noise intensity. We were guided by an early review on statistical processes in neurons[14] and by previous experiments involving external[15,16] or internal[17–19] noise which, in certain cases, was found to enhance some aspect of the quality of the response[15,20]. In an experimental approach similar to the physical demonstrations of SR, we added an external noise source to a weak periodic signal, defining this combination as the stimulus. We obtained both power spectra (PS) and interspike interval histograms (ISIHs), which assess the coherence of the spiking activity with the signal frequency. An alternative measurement, the peri-stimulus time (cycle) histogram, which is sensitive to coherence with the signal phase is not considered here but is being studied in our laboratory.

Original studies of the ISIH of spontaneous and stimulated discharges in cat auditory fibres and their interpretation in terms of a noisy integrate-and-fire model demonstrated the exponential-like decay of peaks located at integer multiples of the stimulus period[21]. Although both single[22–24] and populations[20] of integrate-and-fire models with noise have suggested[25] that neurons can exhibit a noise-enhanced response, these studies did not include a measure of the coherence relative to the noise, which would have been necessary to demonstrate SR. The nature of coherence in the ISIH in periodically forced, noisy, physical systems and its relation to physiological data from similarly forced sensory neurons[19] has recently been discussed[26]. Here we use two separate coherence measurements (the SNR_{PS} and the SNR_{ISIH}, defined below) to demonstrate SR experimentally in single neurons. These SNRs quantify the information content of the spike train without invoking any specific stimulus-encoding mechanism or neuronal model.

Our experiments used near-field mechanoreceptors, located on the crayfish tailfan, in which small motions of cuticular hairs are transduced by their associated sensory neurons into spikes that propagate centrally along the sensory nerves. In power spectra computed from the spikes (Fig. 1), the main feature due to the periodic signal is the narrow peak at the fundamental frequency riding on a broad noise background. This feature was enhanced by intermediate noise intensities (compare Fig. 1*a*, and *b*), but degraded by higher noise intensities (Fig. 1*c*). Interspike internal histograms (Fig. 2) were obtained at the same three external

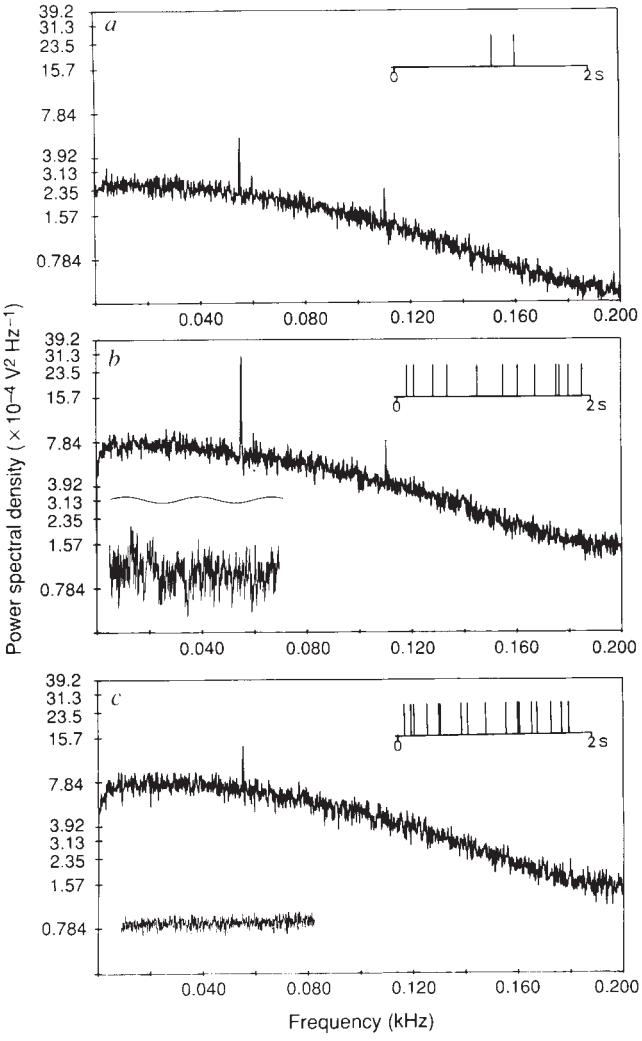

FIG. 1 Power spectra computed from the spiking activity of a crayfish mechanoreceptor, stimulated with a weak signal plus three external noise intensities: *a*, 0; *b*, 0.14; *c*, 0.44 V r.m.s. Insets at upper right show samples of the windowed spike trains from which the power spectra were computed. The total numbers of spikes used for the computations were 698 *a*, 2,390 *b* and 4,031 *c*. All spectra were acquired in the same amount of averaging time, 8.53 min. A single appendage (the telson) was isolated surgically from the crayfish tailfan, together with the associated nerve roots and terminal abdominal ganglion, and immersed in crayfish saline[29] at room temperature. The appendage was mounted vertically on an electromagnetic motion transducer activated by the sum of two inputs: a pure sinusoidal function of 55.2 Hz (the signal), plus a wide-bandwidth gaussian-distributed random function (the noise) as shown in the time series of the signal alone (upper left inset) (*b*) and the signal plus the noise (lower left inset) (*b*) and power spectrum (left inset) (*c*). The sample data shown in the insets were measured for the corresponding conditions stated above for *a*–*c*. The noise shown in the insets is quasi-white but the motion transducer introduced a roll-off of about 6.8 dB per frequency decade. The resulting stimulus was thus a combination of periodic and band-limited random motions of the hair relative to the saline, with the intensities of the noise and signal under independent control. Extracellular recordings from a nerve root were windowed to isolate spikes from a single sensory cell. The windowed events were shaped into 3.5-ms rectangular pulses, passed through a low pass (0–1.5 kHz) filter, and digitized at 10 kHz to obtain power spectra and ISIHs. To maximize the effects of the external noise, mechanoreceptors with low spontaneous spiking rates (low internal noise) were chosen for recording. The entire preparation was mounted on a vibration isolation table, the appendage was rotated so as to select the most effective stimulus direction, and a tuning curve was measured to select the most effective signal frequency. The signal intensity was then set slightly above that required for the minimum detectable SNR_{PS}, and various levels of noise were added to the stimulus. The noise and signal voltages delivered to the electromechanical transducer resulted in a stimulus velocity of 120 μm s^{-1} per V r.m.s. at 10 Hz as determined by an optical calibration. Crayfish mechanoreceptor cells are quite sensitive; without vibration isolation, the cells can easily detect weak building vibrations at 12.5 Hz.

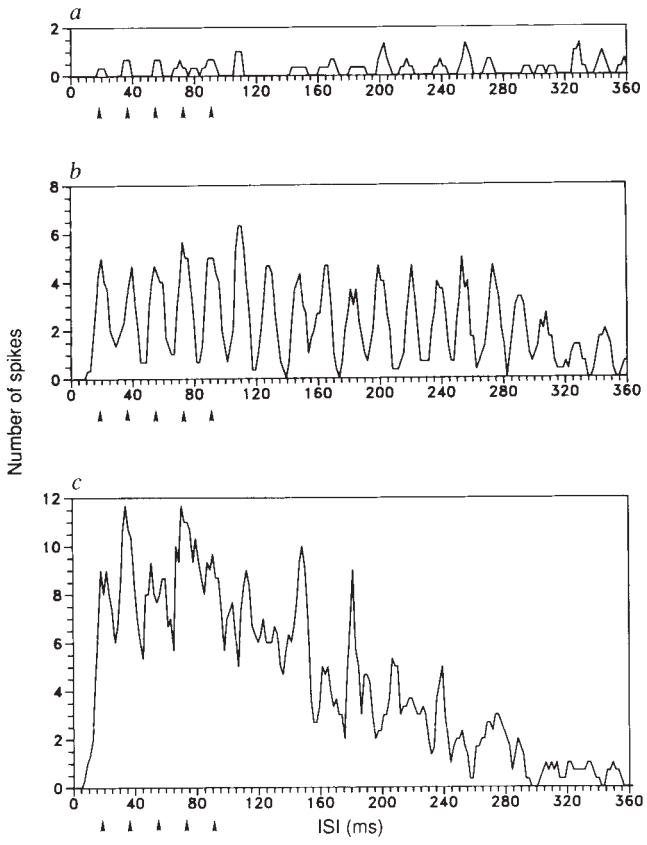

FIG. 2 Interspike interval histograms (ISIHs) obtained under the same conditions used for Fig. 1. To emphasize the coherence of the ISIH peaks with integer multiples of the stimulus period T_0 (18.1 ms), only intervals up to $20T_0$ are shown. Arrowheads mark the first five integer multiples of T_0. For clarity these data were smoothed with a three-point moving average. The SNR_{ISIH} calculations (Fig. 3) were obtained from unsmoothed data. The ISIH shown in *b* does not show the more familiar exponential-like decay of peak amplitudes beyond the first peak because the coherent portion of the stimulus is very weak. Under such conditions it is well known[19] that the histogram is spread out over very long time intervals and that the first peak is not the one of maximum amplitude.

noise intensities. With no external noise (Fig. 2*a*) the spike rate was extremely low and most intervals were longer than those shown in Fig. 2. Intermediate noise (Fig. 2*b*) produced a striking growth of coherence marked by an increase in the amplitude of peaks located at integer multiples of T_0, the stimulus period[26]. Higher noise (Fig. 2*c*) resulted in increasing randomization of the peak structure.

Using various noise intensities, a series of power spectra such as those in Fig. 1 was used to calculate the SNR_{PS} by integrating the data in a small region around the fundamental peak to obtain the strength, S, the area under the signal peak above the noise. The SNR_{PS}, in decibels, was obtained using the standard definition: $SNR_{PS} = 10 \log_{10} [S/N(f_0)]$, where $N(f_0)$ is the amplitude of the broad-band noise background measured at the signal frequency f_0. The results of these measurements (Fig. 3*a*) show a noise-induced signal enhancement of about 4.5 dB at an optimal noise intensity of ~0.14 V r.m.s.

As there is no formal definition of the SNR based on the ISIH, we developed an *ad hoc* definition assuming the occurrences of peaks at integer multiples of T_0 (ref. 26). The interspike intervals located around the first 100 peaks were summed on every interval $iT_0 \pm T_0/4$ for $1 \leqslant i \leqslant 100$, and called N_{max}. Similarly, the remaining intervals located around the troughs were summed on $(i-1/2)T_0 \pm T_0/4$ and called N_{min}. We then defined the $SNR_{ISIH} = 10 \log_{10} (N_{max}/N_{min})^2$. The results (Fig. 3*b*) parallel those computed from the power spectra: a noise-induced enhancement in the SNR_{ISIH} but with a lower optimal noise intensity of ~0.10 V r.m.s.

Not all cells show SR, but we have measured at least some noise-induced enhancement in 10 out of the 11 cells tested. One cell, which had the largest internal noise, $N(f_0)$, showed only a monotonic decline instead of a maximum in the SNR.

Our experiment shows very clearly that weak signals can be enhanced by an optimal level of external noise in single sensory neurons. Does this mean that external noise can help crayfish detect weak signals which they could not detect in its absence? Experiments on sensory interneurons and/or behavioural studies will be necessary to answer this question. But a recent psychophysical experiment[27] and model[28] involving human perception of ambiguous figures in the presence of external noise suggest that this is so. □

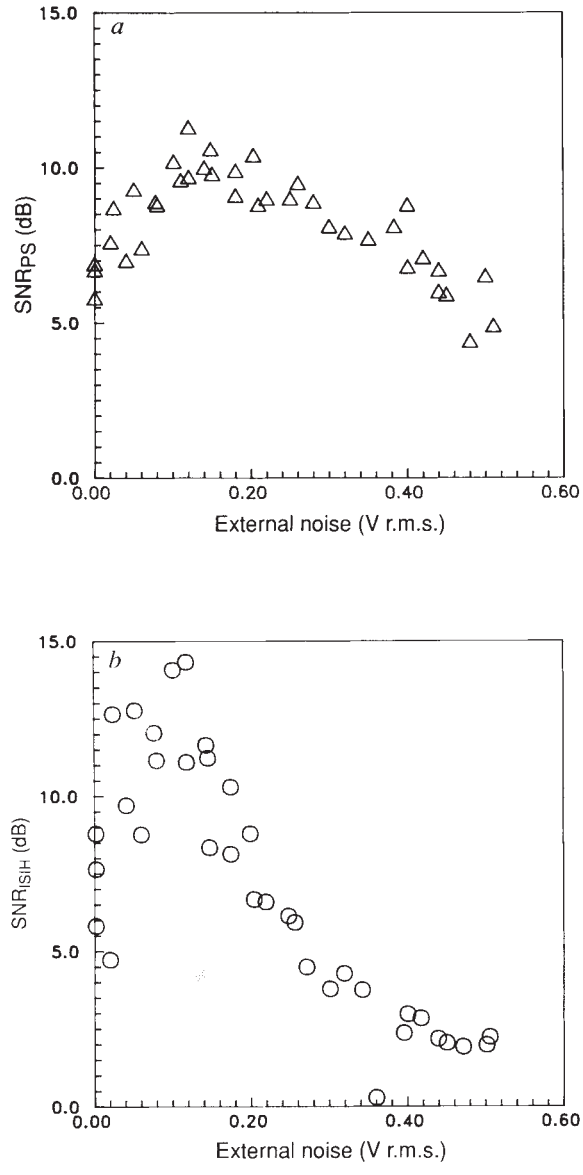

FIG. 3 Stochastic resonance measured from power spectra (*a*) and ISIHs (*b*). The data shown in all figures were acquired from a single representative preparation.

Received 4 March; accepted 6 July 1993.

1. Fauve, S. & Heslot, F. *Phys. Lett.* **97A,** 5–7 (1983).
2. McNamara, B. & Wiesenfeld, K. *Phys. Rev.* A**39,** 4854–4869 (1989).
3. Jung, P. & Hänggi, P. *Europhys. Lett.* **8,** 505–510 (1989).
4. Gammaitoni, L., Marchesoni, F., Meneschella-Saetta, E. & Santucci, S. *Phys. Rev. Lett.* **62,** 349–352 (1989).
5. Moss, F., Bulsara, A. & Shlesinger, M. (eds) *J. stat. Phys.* **70,** 1–514 (1993).
6. Moss, F. in *An Introduction to Some Contemporary Problems in Statistical Physics* (ed. Weiss, G.) (SIAM, Philadelphia, in the press).
7. Benzi, R., Sutera, S. & Vulpiani, A. *J. Phys.* A**14,** L453–L457 (1981).
8. Nicolis, C. *Tellus* **34,** 1–9 (1982).
9. Benzi, R., Parisi, G., Sutera, A. & Vulpiani, A. *Tellus* **34,** 10–16 (1982).
10. Winograd, I. *et al. Science* **258,** 255–260 (1992).
11. Bush, B. M. H. & Laverack, M. S. in *The Biology of Crustacea* Vol. 3 (ed. Bliss, D. E.) 399–468 (Academic, New York, 1982).
12. Mellon, D. *J. exp. Biol.* **40,** 137–148 (1963).
13. Wiese, K. *J. Neurophysiol.* **39,** 816–833 (1976).
14. Moore, G., Perkel, D. & Segundo, J. *A. Rev. Physiol.* **28,** 493–522 (1966).
15. Bañ̃o, W. Jr, Fuentes, J. & Segundo, J. *Biol. Cybern.* **31,** 99–110 (1978).
16. Narins, P. & Wagner, I. *J. acoust. Soc. Am.* **85,** 1255–1265 (1989).
17. Kaplan, E. & Barlow, R. B. Jr *Nature* **286,** 393–394 (1980).
18. Croner, L., Purpura, L. & Kaplan, E. *Proc. natn. Acad. Sci. U.S.A.* **90,** 8128–8130 (1993).
19. Rose, J., Brugge, J., Anderson, D. & Hind, J. *J. Neurophysiol.* **30,** 769–793 (1967).
20. Knight, B. W. *J. gen. Physiol.* **59,** 734–766 (1972).
21. Gerstein, G. & Mandelbrot, B. *Biophys. J.* **4,** 41–68 (1964).
22. Stein, R. B. *Biophys. J.* **5,** 173–184 (1965).
23. Glass, L., Graves, C., Petrillo, G. & Mackey, M. C. *J. theor. Biol.* **86,** 455–475 (1980).
24. Glass, L. & Mackey, M. C. *J. math. Biol.* **7,** 339–352 (1979).
25. Knight, B. W. *J. gen. Physiol.* **59,** 767–778 (1972).
26. Longtin, A., Bulsara, A. & Moss, F. *Phys. Rev. Lett.* **67,** 656–659 (1991).
27. Chialvo, D. & Apkarian, V. *J. stat. Phys.* **70,** 375–392 (1993).
28. Ditzinger, T. & Haken, H. *Biol. Cybern.* **63,** 453–456 (1990).
29. van Harreveld, A. D. *Proc. Soc. exp. Biol. Med.* **34,** 428–432 (1936).

ACKNOWLEDGEMENTS. We thank A. Bulsara for discussions and C. Dames for help with experiments. This work was supported by the US Office of Naval Research.

Induction of human IgE synthesis in B cells by mast cells and basophils

Jean-François Gauchat*, Sybille Henchoz*, Gonzalo Mazzei*, Jean-Pierre Aubry*, Thomas Brunner†, Horst Blasey*, Paul Life*, Dominique Talabot*, Leopoldo Flores-Romo*, Jeff Thompson‡, Kenji Kishi§, Joseph Butterfield‖, Clemens Dahinden† & Jean-Yves Bonnefoy*¶

* Glaxo Institute for Molecular Biology, 14 chemin des Aulx, 1228 Plan-les-Ouates, Geneva, Switzerland
† Inselspital Bern, 3010 Bern, Switzerland
‡ Glaxo Group Research, Greenford UB6 0HE, UK
§ Niigata University School of Medicine, Niigata 951, Japan
‖ Mayo Clinic, Rochester, Minnesota 55905, USA

IMMUNOGLOBULIN E (IgE) is central to the induction of allergic diseases through its binding to the high-affinity receptor (FcεR1) on mast cells and basophils. Crosslinking by allergens of the bound IgE leads to the release of various inflammatory mediators. IgE production by B cells requires a physical interaction with T cells[1], involving a number of surface adhesion molecules[1,2], as well as the soluble factors interleukin-4 (IL-4)[3,4] and IL-13 (ref. 5) produced by T cells[6,7], basophils[8] and mast cells[9]. Here we report that, in the presence of IL-4, mast and basophilic cell lines can provide the cell contact signals that are required for IgE synthesis. The human cell lines HMC-1 (mast) and KU812 (basophilic) both express the ligand for CD40 (CD40L) which is shown to be responsible for the IgE production. Moreover, freshly isolated purified human lung mast cells and blood basophils are also shown to express CD40L and to induce IgE production. This evidence suggests that mast cells and basophils may therefore play a key role in allergy not only by producing inflammatory mediators, but also by directly regulating IgE production independently of T cells.

HMC-1 is an immature mast cell line expressing several mast cell antigens but not FcεR1 (ref. 10). KU812 is an immature basophilic cell line[11]. To identify new cellular mechanisms for the control of IgE production, we tested the ability of these cell lines to induce IgE synthesis in purified B cells stimulated with IL-4 in the absence of T cells. Induction of IgE production and an increase in IgG synthesis was observed when B cells were incubated with HMC-1 or KU812 cells (Fig. 1). IgE production was preceded by a marked increase in IL-4-induced germ-line ε-RNA synthesis (measured at day 5, data not shown).

Studies using anti-CD40 monoclonal antibodies[12,13] and CD40L transfectants[14] indicated that the CD40/CD40L interaction is a key event in the immunoglobulin switching that is required for IgE synthesis. Factors controlling IgE production regulate CD40L expression[15] and T-cell-mediated stimulation of IgE synthesis can be inhibited by soluble forms of CD40 (ref. 16). Furthermore, direct evidence for the importance of CD40L in immunoglobulin switching was provided by the study of patients with hyper-IgM syndrome, which is linked to mutations in CD40L[17–21].

The induction of IgE and the increase in IgG synthesis brought about by HMC-1 or KU812 cells in the presence of IL-4 was inhibited by competition with a chimaeric recombinant fusion protein (Fig. 1) consisting of the extracellular domain of human CD40 fused to a murine IgG constant region (CD40-Fc). No inhibition was observed with the isotype-matched control antibody (Fig. 1). These results show that mast or basophilic cell lines could replace T cells to provide the contact-mediated signal that is required, in conjunction with IL-4, for the induction of IgE production. Inhibition of this production by CD40-Fc indicates an involvement of CD40L.

We investigated whether the expression of CD40L, thus far only detected on T cells[22], could also be observed in HMC-1 or KU812 cells. We found that CD40L was indeed detectable by flow cytometry on both cell lines using fluorescein-labelled CD40-Fc as a probe (Fig. 2). Expression of CD40L was inducible by PMA and ionomycin in HMC-1 and constitutive in KU812 cells (Fig. 2). Expression in HMC-1 and KU812 cells of the messenger RNA coding for CD40L was studied by amplification (polymerase chain reaction) after reverse transcription (RT-PCR) and northern blot assays (Fig. 2). In unstimulated HMC-1, CD40L mRNA could only be detected by RT-PCR. The level of this RNA was maximal after stimulation of HMC-1 cells with calcium ionophore and phorbol ester for 3 hours (Fig. 2 and data not shown). In KU812 cells, there was a low level of constitutive expression of CD40L mRNA, a steady-state level sufficient to maintain detectable CD40L surface expression (Fig. 2). HMC-1 and KU812 CD40L mRNA were amplified after reverse transcription and cloned. Analysis of the sequence of the cloned, amplified complementary DNA, which included all the coding region, indicated that the mRNA coded for a protein identical to the CD40L identified in human T cells (data not shown). Therefore HMC-1 and KU812 cell lines express CD40L which, in conjunction with IL-4, is shown to be able to induce IgE production by B cells.

The immunosupressive drug cyclosporin A (CsA) has recently been shown to be of therapeutic benefit in the treatment of certain atopic diseases[23,24]. We therefore tested the effect of CsA on the up-regulation of CD40L mRNA in HMC-1 cells. When tested at doses similar to those used to demonstrate the effect of this drug on mast cell cytokine production[25], CsA abrogated the stimulation of CD40L mRNA expression induced by calcium ionophore and phorbol ester (Fig. 2*c*) which was paralleled by a decrease in the expression of the corresponding protein

¶ To whom correspondence should be addressed.